NJC

PAPER

View Article Online
View Journal | View Issue

Cite this: *New J. Chem.*, 2018, **42**, 3851

Simple and label-free fluorescence detection of ascorbic acid in rat brain microdialysates in the presence of catecholamines†

Shuyun Zhu, ‡*[ab] Cuihua Lei,‡[a] Yue Gao,[a] Jing Sun,[b] Hongwei Peng,[c] Han Gao,[a] Ruixue Zhang,[a] Rui Wang,[a] Xian-En Zhao*[ab] and Hua Wang *[a]

Ascorbic acid (AA), as one of the most important neurochemicals in cerebral systems, plays a vital role in many physiological and pathological processes. Herein, a facile, label-free, and ultrasensitive fluorescence sensing system was developed for the determination of AA based on the Ag^+–*o*-phenylenediamine (OPD) interaction. OPD could be oxidized by Ag^+ to generate fluorescent 2,3-diaminophenazine (OPDox). When AA was introduced, on the one hand, AA can inhibit the oxidation process due to its strong reducing capability. On the other hand, AA can be oxidized to dehydro-AA with an absorption peak at 380 nm, which has a good spectral overlap with the emission of OPDox. Thus, the inner filter effect (IFE) between dehydro-AA and OPDox may occur. Therefore, the introduction of AA can intensively suppress the fluorescence of the Ag^+–OPD system. Benefitting from the remarkable synergistic effect of the reducing capability of AA and IFE, a facile and ultrasensitive sensor was constructed successfully for AA sensing. The whole detection procedure was achieved within 10 min. The linear response range of AA was obtained from 0.05 to 40 μM with a detection limit of 10 nM. This developed method has many merits including more simplicity, good selectivity, excellent biocompatibility, and more cost-effectiveness without using any nanomaterials. Notably, the proposed method was successfully applied to detect AA in rat brain microdialysates in the presence of catecholamines, thus providing a new route for AA detection in physiological and pathological fields.

Received 23rd November 2017,
Accepted 25th January 2018

DOI: 10.1039/c7nj04574c

rsc.li/njc

1. Introduction

Monitoring the distribution of reactive species in living systems is of great importance for understanding their physiological functions and pathological effects, as well as early stage diagnosis of some serious diseases. Ascorbic acid (AA) is one of the most important neurochemicals in cerebral systems, which plays a vital role in many physiological and pathological processes.[1] Specifically, AA not only functions as an antioxidant in the intracellular antioxidant system but also acts as a neuromodulator for both dopamine- and glutamate-mediated neurotransmissions.[2–5] Moreover, the level of AA is related to some diseases; for instance, the lack of AA will result in scurvy, and excessive intake of AA can lead to urinary stones, diarrhea, and stomach convulsion.[6,7] In this regard, the facile and effective measurements of AA in the cerebral system of living animals are of great physiological and pathological importance and highly desired.[8,9]

Up to now, some analysis methods have been implemented to detect AA such as electrochemistry,[10] capillary electrophoresis,[11] gas chromatography–mass spectrometry,[12] and high-performance liquid chromatography.[13] Although many approaches were well-established, the sophisticated instrumentation, tedious sample preparation, and separation procedures involved might limit their practical applications. To resolve these problems, Mao's group successfully developed electrochemical methods for *in vivo* measurements of AA for the first time.[14] Nevertheless, more simple but effective measurement methods for AA in cerebral systems are still urgently desired.

Fluorescence detection systems have attracted a great deal of interest as a quantitative analytical approach because of their convenient operation, high sensitivity and selectivity, and direct monitoring of target analytes in live cells, tissues, and even animals[15–17] without a complicated pretreated process

[a] *Institue of Medicine and Materials Applied Technologies, College of Chemistry and Chemical Engineering, Qufu Normal University, Qufu City, Shandong Province, 273165, China. E-mail: shuyunzhu1981@163.com, xianenzhao@163.com, huawangqfnu@126.com*

[b] *Qinghai Key Laboratory of Qinghai-Tibet Plateau Biological Resources, Northwest Institute of Plateau Biology, Chinese Academy of Sciences, Xining City, Qinghai Province, 810001, China*

[c] *Hospital of University, Qufu Normal University, Qufu City, Shandong 273165, China*

† Electronic supplementary information (ESI) available. See DOI: 10.1039/c7nj04574c

‡ These authors contributed equally to this work.

and instrumentation during the assay operations. Particularly with the development of nanoscience and nanotechnology, various kinds of nanomaterials have been used as fluorescent probes for the determination of AA. For instance, Tang's group designed cobalt oxyhydroxide (CoOOH)-modified persistent luminescent nanoparticles ($Sr_2MgSi_2O_7$: 1% Eu, 2% Dy) for the determination and screening of AA in living cells and *in vivo* based on the specific reaction of CoOOH.[18] Lin's group designed Fe^{3+}-functionalized carbon quantum dots (CQDs) based on the specific redox reaction between Fe^{3+} and AA for the detection of AA in rat brain microdialysates.[19] They also synthesized tris(hydroxymethyl)aminomethane-derived carbon dot (CD)-modified nanoflakes (tris-derived CD-CoOOH) for monitoring cerebral AA in brain microdialysates.[20] Although these fluorescent nanoprobes displayed good selectivity and sensitivity for the determination of AA in living cells or microdialysates, they are complicated due to the time-consuming synthesis procedure and the complex post-treatment process. In addition, the detection of AA in biological matrices may usually suffer from interferences by catecholamines such as dopamine (DA), norepinephrine (NE), L-levodopa (L-DOPA), epinephrine (EP), 5-hydroxytryptamine (5-HT) and so on. Therefore, it is necessary to develop new methods for the determination of AA in the presence of catecholamines with high selectivity and sensitivity.

In this study, for the first time, we reported a rapid, simple, and novel method for the highly sensitive and selective detection of AA in rat brain microdialysates. As shown in Scheme 1, silver ion (Ag^+), as the oxidase mimic, can catalyze the oxidation of *o*-phenylenediamine (OPD) to form 2,3-diaminophenazine (OPDox) showing strong photoluminescence.[21,22] AA exhibits high reducing capabilities due to its hexose sugar acid with a γ-lactone structure,[23] which could inhibit the generation of luminescent OPDox. Moreover, there is a good spectral overlap between the absorption spectra of the formed dehydro-AA and the emission spectra of OPDox, thus leading to the inner filter effect (IFE). Therefore, the introduction of AA could result in a remarkable decrease in the fluorescence intensity of the Ag^+–OPD system. Based on these facts, a simple and label-free fluorescence method has thus been developed for the detection of AA without the preparation of nanomaterials and the use of expensive instruments. Subsequently, the developed method was successfully applied for the direct analysis of AA in rat brain microdialysates.

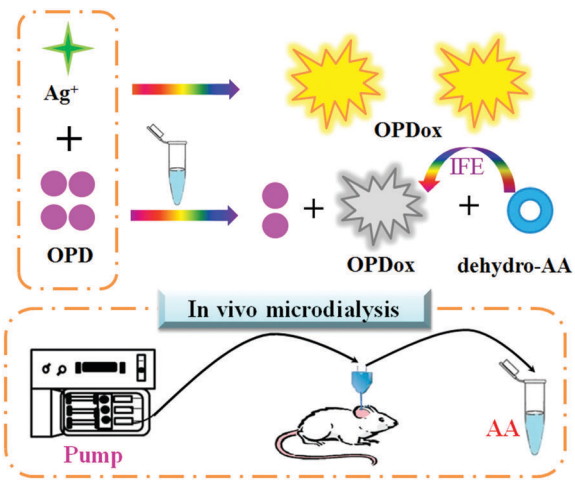

Scheme 1 Schematic illustration of the strategy of facile ascorbic acid sensing.

2. Experimental

2.1. Reagents

Ascorbic acid (AA), dopamine (DA), $AgNO_3$, *o*-phenylenediamine (OPD), hydrogen peroxide (H_2O_2), ethylenediaminetetraacetic acid (EDTA), $Na_2HPO_4{\cdot}12H_2O$, and $NaH_2PO_4{\cdot}2H_2O$ were purchased from Aladdin Company (Shanghai, China). Uric acid (UA), tyrosine (Tyr), serine (Ser), glutamic acid (Glu), lysine (Lys), phenylalanine (Phe), arginine (Arg), glycine (Gly), epinephrine (EP), norepinephrine (NE), levodopa (L-DOPA), dopamine (DA), 5-hydroxytryptamine (5-HT), glutathione (GSH), homocysteine (Hcy), cysteine (Cys), and glucose were purchased from Alfa Aesar. Reduced *N*-ethylmaleimide (NEM) was purchased from Sigma-Aldrich. 10 mM phosphate buffer solution (PBS) was prepared by mixing standard stock solutions of Na_2HPO_4 and NaH_2PO_4. All reagents were of analytical reagent grade, and used as received. Doubly deionized water was used throughout.

2.2. Apparatus

All fluorescence measurements were carried out on an F-7000 spectrometer (Hitachi, Japan) operated at an excitation wavelength at 417 nm. UV-vis spectra were recorded on a UV-vis spectrophotometer (Shimadzu, UV-3600, Japan). *In vivo* microdialysis sampling was accomplished by using a CMA 402 Syringe Pump (CMA, Solna, Sweden) and a CMA 120 System (CMA, Solna, Sweden) for freely moving animals, a microdialysis MAB6 probe (Stockholm, Sweden) which was perfused with Ringer's solution (5 mM) at a flow rate of 2.0 μL min^{-1}, and ASI stereotaxic flat skull coordinates (ASI Instruments Inc., MI, USA).

2.3. Procedure for AA detection

For the detection of AA, 15 μL of 6 mM OPD was diluted in 472 μL of PBS buffer (10 mM, pH 7.0), followed by the addition of 8 μL of 6 mM $AgNO_3$, and then 5 μL of different concentrations of AA. The samples were incubated for 10 min in the dark at room temperature before fluorescence measurements. The selectivity of AA was explored in a similar way by adding other interferences. The fluorescence spectra were collected upon excitation at 417 nm, and the slit wavelengths of both excitation and emission were 5 nm, respectively.

2.4. Detection of AA in rat brain microdialysates

In vivo microdialysis experiments were performed as our previous work.[24,25] Briefly, the rats were anesthetized with 20% urethane (1.2 g kg^{-1}, i.p.) before probe implantation surgery, and remained anesthetized throughout the experimental period. The rat's body temperature was maintained at 37 °C during the experimental procedure. A pretreated probe was inserted into the

right striatum with stereotaxic flat skull coordinates: A: +1.0 mm from bregma, L: ±2.9 mm from midline and H: −3.5 mm from dura. The animals were awake and freely moving with access to food and water throughout the experiment. Next, the brain microdialysis probe (MAB6) was perfused with artificial cerebrospinal fluid (aCSF) (126 mM NaCl, 27.5 mM $NaHCO_3$, 2.4 mM KCl, 1.1 mM $CaCl_2$, 0.85 mM $MgCl_2$, 0.5 mM Na_2SO_4, 0.5 mM KH_2PO_4, and pH = 7.0) at a rate of 2.0 μL min^{-1} using a microinjection pump (CMA 402, Sweden) and a microsyringe (CMA, 1.0 mL) for 90 min to reach baseline values. Finally, every 50 μL of microdialysate was collected for the following AA sensing.

3. Results and discussion

3.1. Design and establishment of an AA sensing system

As shown in Fig. 1, the aqueous solution of OPD has always remained colorless and exhibited negligible fluorescence (curve and vial 1). In contrast, the introduction of Ag^+ essentially triggers the oxidative reaction of OPD, during which the original colorless and non-fluorescent solution gradually turned to pale yellow in color and showed intense orange-yellow fluorescence under ultraviolet (curve and vial 2). As shown in Fig. 1A, the Ag^+–OPD mixed solution has an obvious absorption peak at about 417 nm, which belongs to the characteristic absorption spectrum of OPDox, the main oxidation product of OPD.[26] Meanwhile, the corresponding emission spectrum in Fig. 1B exhibited a peak at about 557 nm, which is similar to that of OPDox in previous studies as well.[27,28] Then, both the absorption intensity at 417 nm and the fluorescence intensity at 557 nm decreased obviously after the addition of AA (curve and vial 3).

In order to verify the sensing mechanism, the addition sequence of AA was investigated. As shown in Fig. S1 (ESI†), Ag^+ could oxidize OPD to generate OPDox with strong fluorescence (curve a). According to the previous report,[21] Ag^+ was reduced to zero-valent silver and formed silver nanoparticles (AgNPs). Actually, the formed nanoparticles were observed on a membrane layer by TEM analysis (Fig. S2A, ESI†). To confirm the components that might comprise such nanoparticles, the thus-formed nanoparticles were characterized by energy-dispersive spectroscopy (EDS) analysis. As shown in Fig. S3 (ESI†), the element present in the nanoparticles was silver. These results indicated that the formation of AgNPs could occur during the reaction of Ag^+ and OPD. After AA was added to the Ag^+–OPD mixed solution, the fluorescence intensity of the solution decreased remarkably (curve b), indicating that AA could reduce fluorescent OPDox into non-fluorescent OPD. It has also been reported that AA was a common reducing agent for the synthesis of AgNPs.[29] So, AA was reacted firstly with Ag^+ for 5 min followed by the addition of OPD. As shown in curve c of Fig. S1 (ESI†), the fluorescence intensity of the solution decreased further. Moreover, the formed AgNPs exhibited different sizes and morphologies (Fig. S2B, ESI†). The results indicated that AA was also responsive to Ag^+. Therefore, the presence of AA inhibited the generation of OPDox due to its strong reducibility towards both OPDox and Ag^+. More interestingly, a new absorption peak generated at 380 nm from the formed dehydro-AA had a good overlap with the excitation spectrum of fluorescent OPDox (Fig. S4, ESI†), resulting in the occurrence of the inner filter effect (IFE). Owing to the two reasons, the significant enhancement in the fluorescence along with the oxidative reaction of OPD could be partially suppressed in the presence of AA.

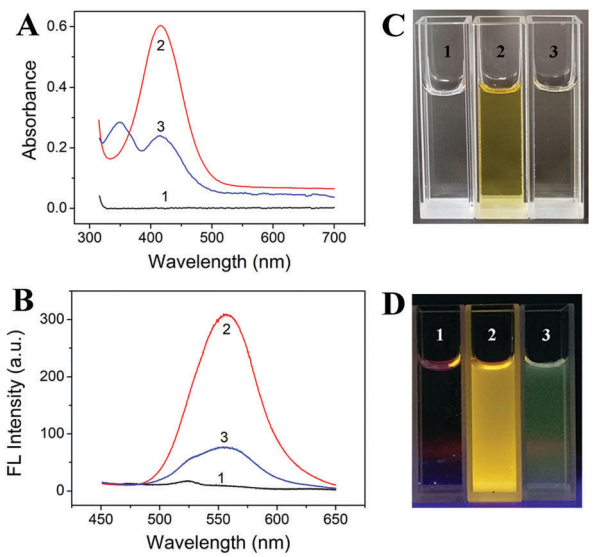

Fig. 1 Absorbance (A) and fluorescence emission spectra (B) of the OPD (1), OPD + Ag^+ (2), and OPD + Ag^+ + AA in PBS buffer at pH 7.0. The corresponding photographs under visible (C) and ultraviolet light (D). The final concentrations of OPD, Ag^+, and AA are 180 μM, 96 μM, and 30 μM, respectively.

Catecholamines, as common interferences, usually coexist in biological fluids with AA. Therefore, we investigated the influences of catecholamines including DA, EP, NE, L-DOPA, and 5-HT on the fluorescence responses of the Ag^+–OPD system. As shown in Fig. S5 (ESI†), the fluorescence intensity decreases up to 80% at 30 μM AA. In contrast, the presence of 30 μM catecholamines resulted in less than 20% fluorescence quenching. Similarly, the extent of the decrease of the absorption intensity at 417 nm in the presence of catecholamines was less than that of AA. Besides, no new absorption peak was observed after the addition of catecholamines. These results indicated that AA possesses a high inhibition efficiency towards the fluorescence intensity of Ag^+–OPD system due to the synergistic effect of a stronger reducibility of AA and IFE. Therefore, a convenient fluorimetric assay could be designed for sensing AA sensitively and selectively.

3.2. Optimization of the sensing system

The reaction conditions were optimized to establish the optimum analytical conditions. pH is a crucial factor for almost every sensing system. Fig. 2A shows the fluorescence intensity of the Ag^+–OPD system in the presence and absence of AA in the media with different pH values. The fluorescence intensity showed the largest difference when the pH was around 7.0. In the strong acidic medium, the amino groups of OPD could be protonated, which could inhibit the oxidation by Ag^+. When the pH value was higher than 7.0, Ag^+ might be more prone to hydrolysis, which

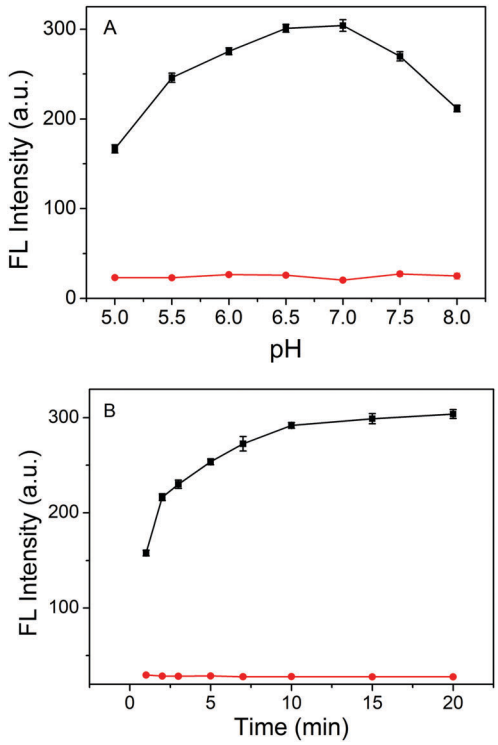

Fig. 2 Effects of pH (A) and reaction time (B) on the fluorescence intensity at 557 nm in the absence (■) and presence (●) of 40 μM AA. Other conditions are the same as those shown in Fig. 1.

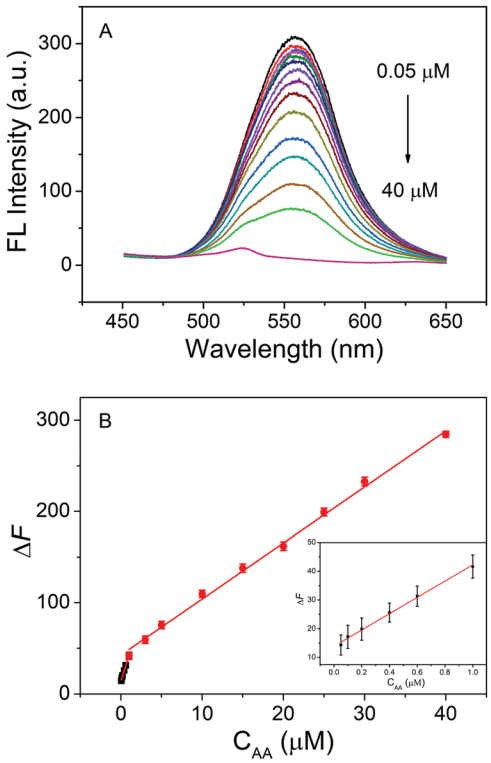

Fig. 3 (A) Fluorescence spectra of the Ag^+–OPD solution in the presence of varied concentrations of AA (0–40 μM). (B) Relationship between ΔF and the concentrations of AA. Inset: Relationship between ΔF and the lower concentrations of AA.

could decrease its oxidization ability. Moreover, a pH of 7.0 was established to fit for the enzyme mimetic reaction. Therefore, pH 7.0 was the optimal condition for the sensing system.

The effect of reaction time on the detection of AA was also studied, and the experimental results are shown in Fig. 2B. The results indicated that the fluorescence of the Ag^+–OPD system increased gradually and reached about 90% of the maximum when the reaction time reached 10 min, showing that the oxidation reaction was almost complete in 10 min. While in the presence of AA, the fluorescence decreased quickly in the first 1 min, and then remained almost constant in the following 20 min. Thus, the optimum time for the proposed system was set as 10 min.

3.3. Sensitivity of the sensing system

Under the optimized conditions, we evaluated the analysis capability of this system for the quantitative detection of AA. As shown in Fig. 3A, it was clearly seen that with the increase of AA concentrations, the fluorescence intensities of the Ag^+–OPD system decreased gradually while $\Delta F = F_0 - F$ increased systematically, where F_0 and F are the fluorescence intensities at 557 nm in the absence and presence of AA, respectively. The ΔF exhibited a good linear relationship with AA in the two concentration ranges of 0.05–1.0 μM and 1.0–40 μM. The regression equations were $\Delta F = 13.88 + 28.39C_{AA}$ (μM) ($R^2 = 0.995$) and $\Delta F = 42.56 + 6.147C_{AA}$ (μM) ($R^2 = 0.997$), respectively. The detection limit can reach as low as 10 nM estimated by a signal to noise ratio of 3. Moreover, the analysis repeatability of the proposed method was evaluated by six repeated measurements of 0.5 μM and 5.0 μM AA and the relative standard deviation (RSD) was 3.61% and 2.37%, respectively, demonstrating the reliability of the proposed method.

In addition, we compared the characteristics of the proposed sensor with other fluorescent AA sensors reported elsewhere. As shown in Table 1, this proposed system could provide better detection sensitivity in comparison with those of other fluorescent nanoprobes including gold nanoclusters,[30] carbon quantum dots (CQDs),[31] graphitic carbon nitride nanosheets,[32] copper nanoclusters,[33] and graphene quantum dots (GQDs).[23] Moreover, this developed fluorimetric method is relatively simple and fast, in which the whole detection procedure can be finished within 10 min. In contrast, fluorescent nanomaterials may entail a much longer reaction time for preparation by using the complicated synthesis and post-treatment process.

3.4. Selectivity of the Ag^+–OPD system with different ions and biological molecules

To evaluate the specificity of the developed assay for AA, several potential interfering compounds were investigated under the same conditions. Firstly, various metal ions including K^+, Ca^{2+}, Zn^{2+}, Mg^{2+}, Na^+, Mn^{2+}, Ba^{2+}, Co^{2+}, and Cu^{2+} containing the Ag^+–OPD system were measured upon excitation at 417 nm. As demonstrated in Fig. 4A, these potential metal ions caused no significant signal fluctuations, indicating that they showed negligible influence on the fluorescence intensity of the Ag^+–OPD system.

Table 1 Comparison of detection performances for AA among different probes

Probes/ref.	Linear range (μM)	Detection limit (μM)	Synthesis time for probes
Protein-modified Au nanoclusters/30	1.5–10	0.2	24 h
Phosphorus/nitrogen dual-doped CQDs[a]/31	5–200	1.35	72 h
Graphitic carbon nitride nanosheets/32	0.5–200	0.13	24 h
Cu nanoclusters/33	0.5–10	0.11	6 h
GQDs[b]/23	0.5–250	0.28	28 h
Hexagonal cobalt oxyhydroxide–carbon dots/34	0.1–20	0.05	40 min
CdS QDs/35	0.06–0.3	0.002	1 h
Ag^+–OPD/this work	0.05–1.0 1.0–40	0.01	10 min

[a] Carbon quantum dots. [b] Graphene quantum dots.

Usually the concentration of catecholamines in biological fluids is much lower than that of AA. Thus, the selectivity of the Ag^+–OPD system was further validated by comparing the signal changes of samples containing the lower concentrations of catecholamines and other common biological molecules. As shown in Fig. 4B, except for GSH, Hcy, and Cys, the response of the Ag^+–OPD system was selective toward AA. Because GSH, Hcy, and Cys could also have somewhat reducing abilities towards Ag^+, their addition resulted in the decrease of the fluorescence. However, *N*-ethylmaleimide (NEM), a scavenger that can exclusively react with a sulfhydryl compound, could effectively eliminate the interference.[36] As can be seen from Fig. 4B, after incubation of GSH, Hcy, or Cys with NEM, the Ag^+–OPD system did not cause obvious fluorescence decrease, whereas the determination of AA was not affected by the introduction of NEM. Therefore, the Ag^+–OPD system could present a sensitive and selective fluorescence approach toward AA sensing by employing NEM as an effective GSH, Hcy, and Cys scavenger.

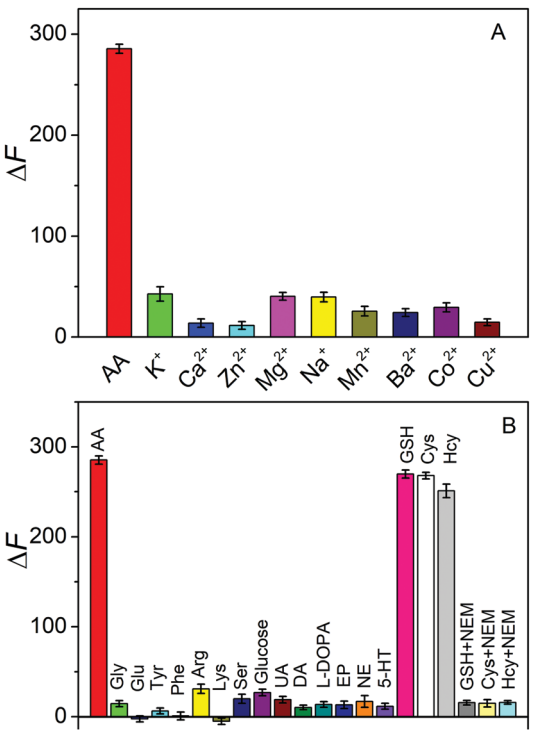

Fig. 4 (A) The selectivity of the Ag^+–OPD system towards different metal ions. The concentration of AA is 40 μM, and the concentration of all the metal ions is 400 μM. (B) The selectivity of the Ag^+–OPD system towards other biological molecules. The concentration of AA is 40 μM, and the concentrations of UA, DA, L-DOPA, NE, and EP are 5 μM, respectively. The concentrations of other interfering species are 40 μM. The NEM concentration is 0.3 mM.

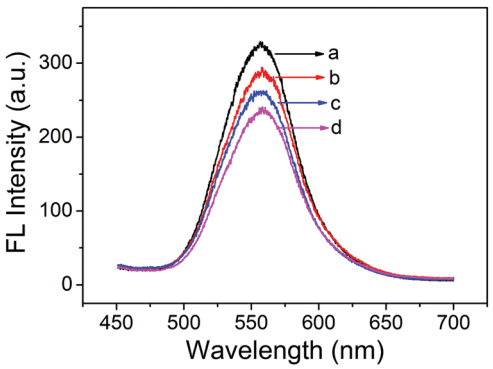

Fig. 5 Fluorescence spectra of the Ag^+–OPD system for AA detection in rat brain microdialysates: the Ag^+–OPD system (a); the successive addition of 50 μL of microdialysates (b), 5 μL of AA solution (c), and 5 μL of AA solution (d).

3.5. Application of the proposed sensing system to rat brain microdialyate analysis

Recently, AA has been proven to be a kind of neuromolecule, thus monitoring the levels of AA in brain microdialysates is important for research on physiology, pathology, and clinics. In our experiment, an unknown amount of AA in a rat brain microdialysis sample was estimated by using the standard addition method with 0.5 μM AA solution. As shown in Fig. 5, the fluorescence spectra of the Ag^+–OPD system were recorded in the absence (a) and presence of 50 μL rat brain microdialysates (b). Next, 5 μL of 50 μM AA standard solution was added twice (curves c and d, Fig. 5). According to the standard method, the concentration of AA was calculated to be 5.96 μM in the rat brain microdialysates, which is consistent with previous reports.[37]

4. Conclusions

In summary, a novel fluorescence assay was developed for the facile detection of AA based on the synergistic effect of reducing

ability of AA and IFE. The Ag^{+}–OPD probing system features some excellent chemical properties such as high water solubility and strong fluorescence intensity, which could be served as a novel fluorescence probe for AA sensing. Moreover, no nanomaterials participated in the assays, making it a simple, cost-effective, fast, and less laborious candidate. More importantly, this fluorimetric method was successfully applied for the determination of AA in rat brain microdialysates samples, providing a potential platform for AA monitoring from many other biological samples.

Conflicts of interest

There are no conflicts to declare.

Acknowledgements

This work is kindly supported by the National Natural Science Foundation of China (No. 21405094, 21775088, and 21675099), the Open Funds of the State Key Laboratory of Electroanalytical Chemistry (No. SKLEAC201506), the Natural Science Foundation of Qinghai Province (2016-ZJ-955), the Development Project of Qinghai Key Laboratory (No. 2017-ZJ-Y10), the National Undergraduate Research Training Program (No. 201610446033 and 2017A029), and the Scientific Research Foundation of Qufu Normal University (No. BSQD201203).

Notes and references

1 Y. Li and X. Lin, *Sens. Actuators, B*, 2006, **115**, 134.
2 X. Gao, P. Yu, Y. Wang, T. Ohsaka, J. Ye and L. Q. Mao, *Anal. Chem.*, 2013, **85**, 7599.
3 K. Liu, P. Yu, Y. Wang, T. Ohsaka and L. Q. Mao, *Anal. Chem.*, 2013, **85**, 9947.
4 Y. Lin, P. Yu, J. Hao, Y. Wang, T. Ohsaka and L. Q. Mao, *Anal. Chem.*, 2014, **86**, 3895.
5 M. E. Rice, *Trends Neurosci.*, 2000, **23**, 209.
6 S. J. Padayatty, A. Katz, Y. Wang, P. Eck, O. Kwon, J. H. Lee, S. Chen, C. Corpe, A. Dutta, S. K. Dutta and M. Levine, *J. Am. Coll. Nutr.*, 2003, **22**, 18.
7 M. Sönmeza, G. Türk and A. Yüce, *Theriogenology*, 2005, **63**, 2063.
8 T. Finkel and N. J. Holbrook, *Nature*, 2000, **408**, 239.
9 M. E. Rice, *Trends Neurosci.*, 2000, **23**, 209.
10 S. Y. Zhu, H. J. Li, W. X. Niu and G. B. Xu, *Biosens. Bioelectron.*, 2009, **25**, 940.
11 N. B. Saari, A. Osman, J. Selamat and S. Fujita, *Food Chem.*, 1999, **66**, 57.
12 W. D. Mark, B. Guy and V. M. Marc, *Anal. Biochem.*, 1996, **239**, 8.
13 M. Yuta, Y. Mayumi, Y. Toshihide, M. Fumiya and Y. Kenichi, *Free Radical Biol. Med.*, 2012, **53**, 2112.
14 M. Zhang, K. Liu, L. Xiang, Y. Lin, L. Su and L. Mao, *Anal. Chem.*, 2007, **79**, 6559.
15 S. Y. Zhu, L. He, F. Zhang, M. Y. Li, S. L. Jiao, Y. Li, M. Y. Chen, X. E. Zhao and H. Wang, *Talanta*, 2016, **161**, 169.
16 S. S. Ma, Y. X. Qi, X. Q. Jiang, J. Q. Chen, Q. Y. Zhou, G. Y. Shi and M. Zhang, *Anal. Chem.*, 2016, **88**, 111647.
17 X. E. Zhao, C. H. Lei, Y. Gao, H. Gao, S. Y. Zhu, X. Yang, J. M. You and H. Wang, *Sens. Actuators, B*, 2017, **253**, 239.
18 N. Li, Y. Li, Y. Han, W. Pan, T. Zhang and B. Tang, *Anal. Chem.*, 2014, **86**, 3924.
19 L. B. Li, C. Wang, J. X. Luo, Q. W. Guo, K. Y. Liu, K. Liu, K. Liu, W. J. Zhao and Y. Q. Lin, *Talanta*, 2015, **144**, 1301.
20 L. B. Li, C. Wang, K. Y. Liu, Y. H. Wang, K. Liu and Y. Q. Lin, *Anal. Chem.*, 2015, **87**, 3404.
21 X. Yang and E. K. Wang, *Anal. Chem.*, 2011, **83**, 5005.
22 H. C. Dai, P. J. Ni, Y. J. Sun, J. T. Hu, S. Jiang, Y. L. Wang and Z. Li, *Analyst*, 2015, **140**, 3616.
23 F. P. Shi, Y. Zhang, W. D. Na, X. Y. Zhang, Y. Li and X. G. Su, *J. Mater. Chem. B*, 2016, **4**, 3278.
24 Y. R. He, X. E. Zhao, S. Y. Zhu, N. Wei, J. Sun, Y. B. Zhou, S. Liu, Z. Q. Liu, G. Chen, Y. R. Suo and J. M. You, *J. Chromatogr. A*, 2016, **1458**, 70.
25 X. E. Zhao, Y. R. He, P. Yan, N. Wei, R. J. Wang, J. Su, L. F. Zheng, S. Y. Zhu and J. M. You, *RSC Adv.*, 2016, **6**, 108635.
26 S. S. Ma, Q. Y. Zhou, F. Y. Mu, Z. H. Chen, X. Y. Ding, M. Zhang and G. Y. Shi, *Analyst*, 2017, **142**, 3341.
27 J. Sun, B. Wang, X. Zhao, Z. J. Li and X. R. Yang, *Anal. Chem.*, 2016, **88**, 1355.
28 R. Li, C. H. Lei, X. E. Zhao, Y. Gao, H. Gao, S. Y. Zhu and H. Wang, *Spectrochim. Acta, Part A*, 2018, **188**, 20.
29 S. P. Wu and S. Y. Meng, *Mater. Chem. Phys.*, 2005, **89**, 423.
30 X. Wang, P. Wu, X. Hou and Y. Lv, *Analyst*, 2013, **138**, 229.
31 X. J. Gong, Y. Liu, Z. H. Yang, S. M. Shuang and Z. Y. Zhang, *Anal. Chim. Acta*, 2017, **968**, 85.
32 M. C. Rong, L. P. Lin, X. H. Song, Y. R. Wang, Y. X. Zhong, J. W. Yan, Y. F. Feng, X. Y. Zeng and X. Chen, *Biosens. Bioelectron.*, 2015, **68**, 210.
33 H. B. Rao, H. W. Ge, Z. W. Lu, W. Liu, Z. Q. Chen, Z. Y. Zhang, X. X. Wang, P. Zou, Y. Y. Yang, H. He and X. Y. Zeng, *Microchim. Acta*, 2016, **183**, 1651.
34 L. B. Li, C. Wang, K. Y. Liu, Y. H. Wang, K. Liu and Y. Q. Lin, *Anal. Chem.*, 2015, **87**, 3404.
35 M. Ganiga and J. Cyriac, *Anal. Bioanal. Chem.*, 2016, **408**, 3699.
36 Y. Cen, J. Tang, X. J. Kong, S. Wu, J. Yuan, R. Q. Yu and X. Chu, *Nanoscale*, 2015, **7**, 13951.
37 R. Liu, D. Wu, S. Liu, K. Koynov, W. Knoll and Q. Li, *Angew. Chem., Int. Ed.*, 2009, **48**, 4598.

